Rr Study Appendix C

Choosing a radius for the integration surface

The focus of the article is on determining Rr and Rg given the power delivered to the feed-point (Pi). Using E and H-field amplitudes and phases derived from NEC modeling we can determine the power density distribution on a surface. By integrating the power density over that surface we can directly determine either Pr or Pg which allows us to separate Pr and Pg from Pi which, when combined with Io, allows us to determine Rr and Rg. In free space the radial distance from the antenna to the surface of integration doesn't matter, you'll get the same value for **Rr** in any case. However, in this study we want to include what are typically called "ground" or "soil" losses which lie inside the power integration surface and designate them as **Rg**. The power which passes through the surface is associated with **Rr**. The problem is that you will accrue some additional loss no matter what radius you choose initially when that radius is increased. By convention some of these losses are considered to be "far-field" losses which are not part of **Rg**. Unfortunately the fields close to the antenna have exponentially decaying terms proportional to $1/r$, $1/r^2$, $1/r^3$, so the regions blend gradually into each other without sharp distinctions. This is particularly the case for the boundary between the reactive near-field and the Fresnel zone. While most antenna books will have at least a brief discussion of the field zones, for the most part these are very general with limited detail. Kraus[1] suggests a near-field/Fresnel boundary at a radius of one radian ($\lambda/2\pi \approx 0.16\lambda$) as shown in figure C1.

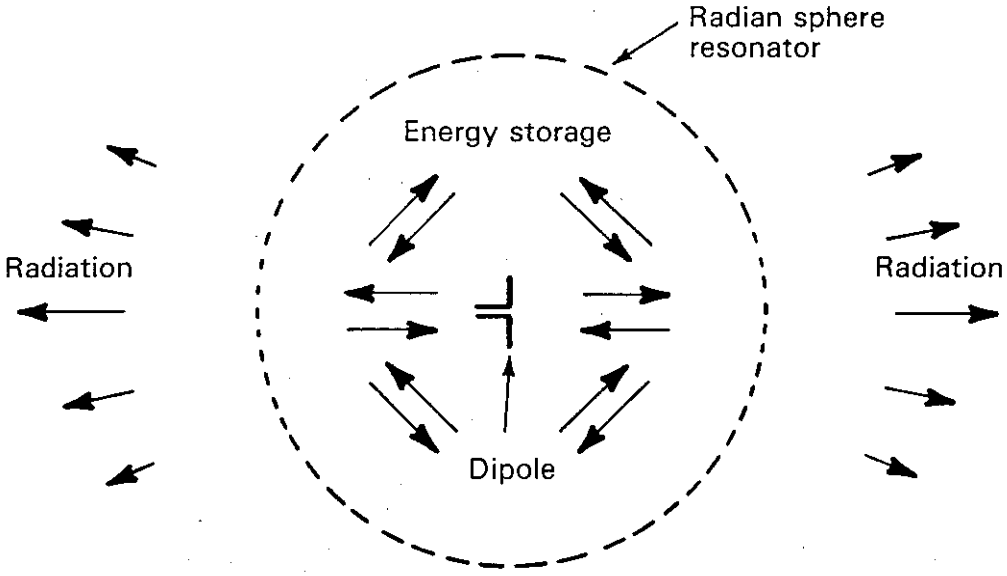

Figure C1 - Radian sphere concept from Kraus[1].

Kraus[1] derives his boundary radius from an analysis of a very short (L<<λ) dipole with a uniform current and gives the following equations for |Ez| and $|H\varphi|$ at the ground surface:

$$|Ez| = \frac{IohZo}{\lambda}\left(\frac{j}{2r} + \frac{1}{4\pi r^2} - \frac{j}{8\pi^2 r^3}\right) = \frac{IohZo}{\lambda}(jA + B - jC) \quad (1)$$

$$|H\varphi| = \frac{Ioh}{\lambda}\left(\frac{j}{2r} + \frac{1}{4\pi r^2}\right) \quad (2)$$

Where Zo is 377Ω, h is the height in wavelengths (<<1), the current is assumed uniform along h and r is the radius from the antenna in wavelengths. The magnitudes of A, B and C in equation (1) are compared in figure C3.

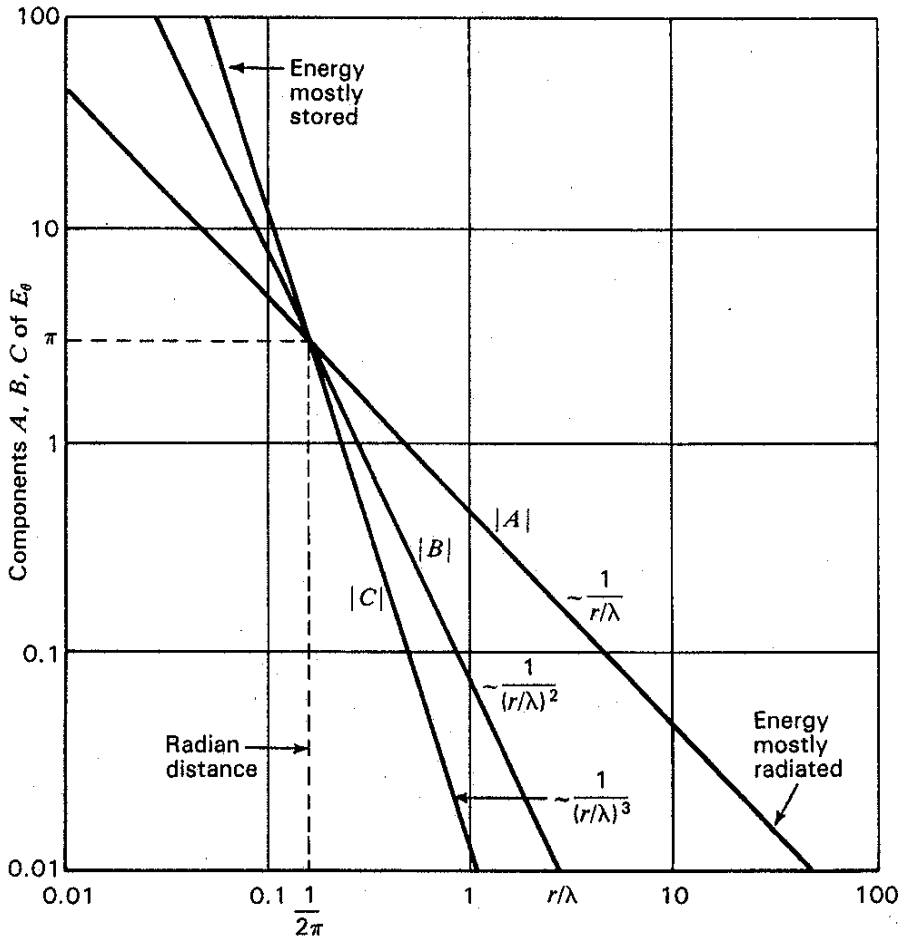

Figure 5-6 Variation of the magnitudes of the components of E_θ of a short electric dipole as a function of distance (r/λ). The magnitudes of all components equal π at the radian distance $1/(2\pi)$. At larger distances energy is mostly radiated, at smaller distances mostly stored.

Figure C2 - Kraus[1] field amplitudes.

Figure C2 predicts that |Ez| close the antenna will fall ≈$1/r^3$ but at larger distances |Ez| is asymptotic to 1/r. Notice that for $r<1/2\pi$ the energy is mostly stored but for $r>>1/2\pi$ it is mostly radiated. In between the energy is some combination of the two. This illustrates the arbitrariness in defining the boundary between the reactive near-field and Fresnel zones. However, for more realistic antennas the fields can be different.

There is a careful, quantitative discussion of the field zones around and antenna in Constantine Balanis's book "Antenna Theory"[2]. The following definitions are taken verbatim from his work. Figure C3 shows the field regions in a general way along with expressions for the applicable radii.

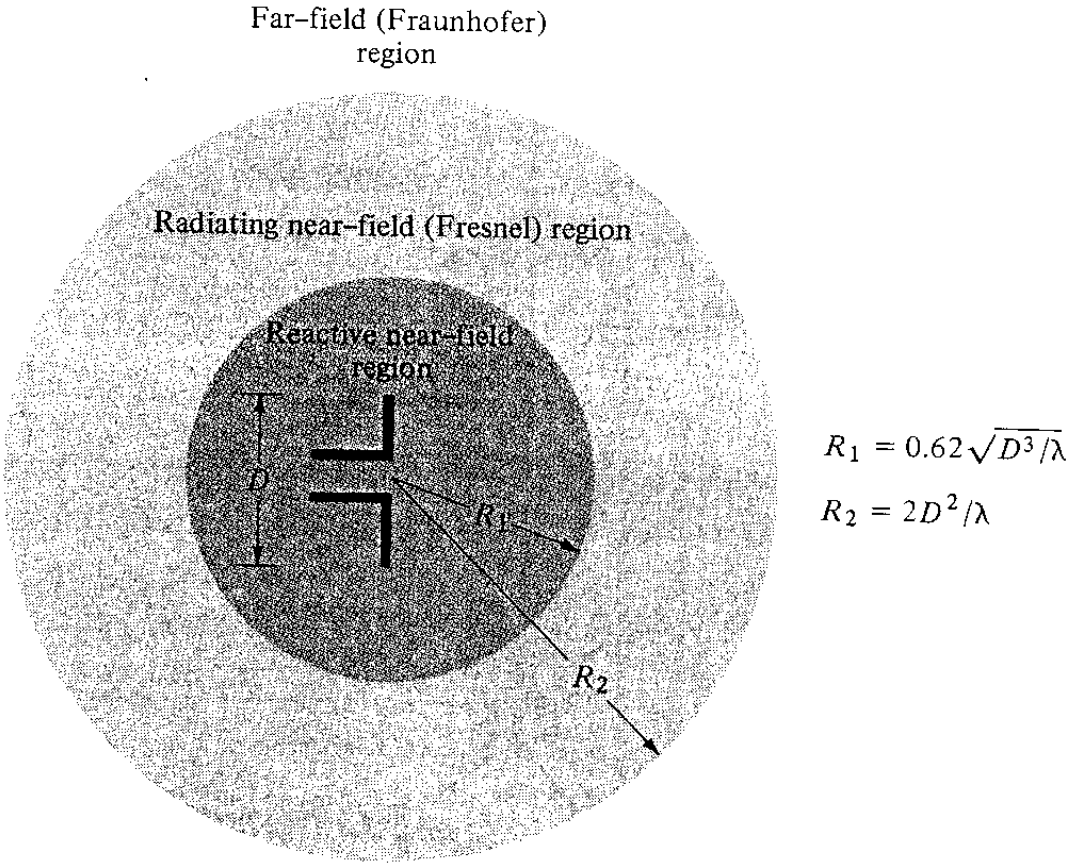

Figure C3 - Field zones (From Balanis [2])

Balanis defines the field regions as follows:

"The space surrounding an antenna is usually subdivided into three regions: (a) reactive near-field, (b) radiating near-field (Fresnel) and (c) far-field (Fraunhofer) regions.....Although no abrupt changes in the field configurations are noted as the boundaries are crossed, there are distinct differences among them. The boundaries separating these regions are not unique, although various criteria have been established and are commonly used to identify the regions.

The reactive near-field region is defined as "that region of the field immediately surrounding the antenna wherein the reactive field predominates. For most antennas, the outer boundary of this region is commonly taken to exist at of distance $R < 0.62\sqrt{D^3/\lambda}$ *from the antenna surface, where λ is the wavelength and D is the largest dimension of the antenna."*

"The Radiating near-field (Fresnel) region is defined as "that region of the field of an antenna between the reactive near-field region and the far-field region wherein radiation fields predominate and wherein the angular field distribution is dependent upon the distance from the antenna. ..... The inner boundary is taken to be $R \geqq 0.62\sqrt{D^3/\lambda}$ *and the outer boundary distance* $R<2D^2/\lambda$."

"The far-field (Fraunhofer) region is defined as that region of the field of an antenna where the angular field distribution is essentially independent of the distance from the antenna. ....The inner boundary is taken to be the radial distance $R=D^2/\lambda$."

When we apply these boundaries to monopoles close to ground D = twice the height of the vertical because it includes the image. For example if h=0.25λ then D=0.5λ and R_1 ≈ 0.22λ which is not greatly different from Kraus's value of 0.16λ. In a footnote Balanis adds a caveat: strictly speaking these boundary limits apply for antennas where D>λ. We are discussing antennas smaller than this so the limits become even more approximate!

Analysis options

To determine a meaningful values for Rr and Rg we need to decide what radius to use for the integration cylinder. Ideally we would like that to be the boundary between the reactive near-field and Fresnel zones but the transition between the two zones is gradual without a sharp boundary. At best any value we choose will be approximate. To guide us in the choice of radius there are a number of things we might look at:

1) E_z with distance from the base.

2) H_y with distance from the base.

3) The ratio E_z/H_y which is the wave impedance Z. For a plane wave in free space Z=Zo=376.8Ω.

4) Rr with distance from the base.

5) Total power dissipation in the soil within a given radius.

In the sections which follow we will look at each of these options and in the end make a judgment call.

E_z and H_y graphs

There are a couple of ways can obtain values for Ez and Hφ, from a NEC model or from theoretical equations. The way I've proceeded is to use NEC as my primary source but check the NEC results against the equations.

Equations (1) and(2) are for very short verticals (h<<1). For h=λ/4 with a sinusoidal current distribution the equations are somewhat simpler:

$$|Ez| = \frac{IohZo}{2\pi\lambda\sqrt{0.25^2+r^2}} \quad (3)$$

$$|H\varphi| = \frac{Ioh}{2\pi\lambda r} \quad (4)$$

Figure C4 shows a comparison between NEC and equation (3).

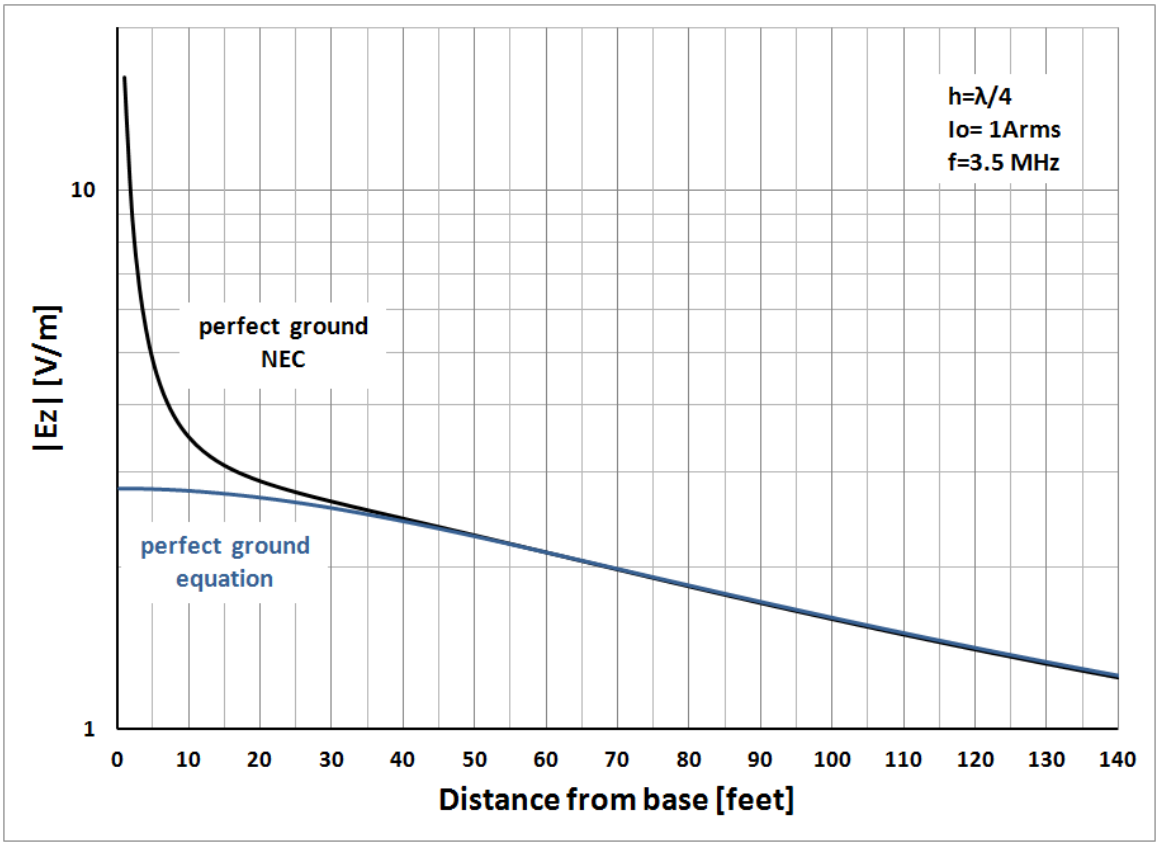

Figure C4 - comparison of Hφ at z=0 between NEC and equation (3).

While there is close agreement between the graphs for r>30', inside that distance the field values diverge. This is an illustration of why I prefer to use NEC for the field values, at least close to the base. The classical equations do not take into account the voltage across the feedpoint which can be very substantial, particularly in short loaded verticals but NEC does. This point is often overlooked in antenna texts! This becomes even more important when analyzing verticals over real ground with actual ground systems. Figure C5 illustrates this.

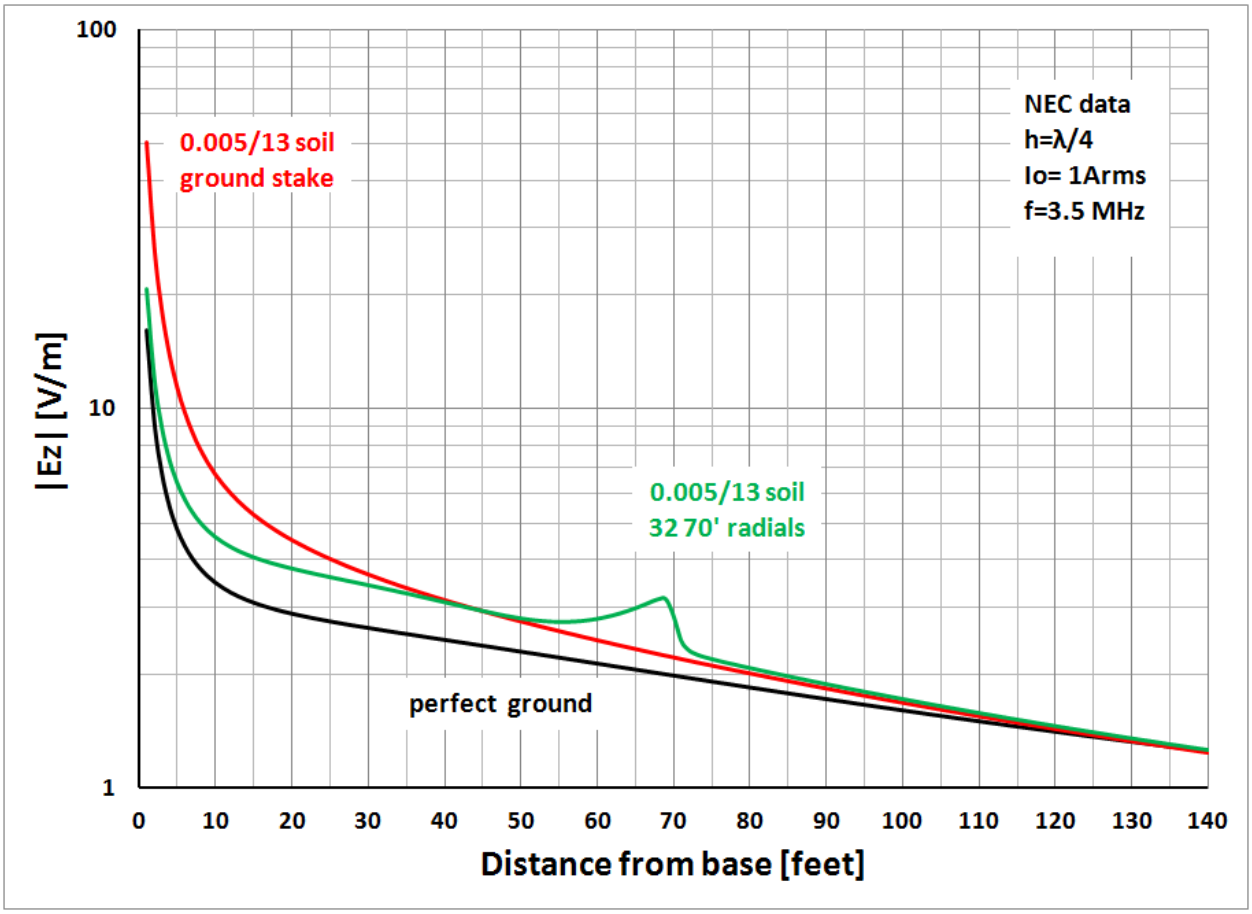

Figure C5 - Comparison of Ez values derived from NEC for different ground system arrangements.

Notice the differences in |Ez| close to the base. When we go from perfect ground to real grounds with a ground system the input impedance at the feedpoint increases due to the addition of the ground loss term Rg. For the same current (Io=1Arms in this example) this will increase the voltage across the feedpoint which increases |Ez|. It should be noted that a comparison between NEC and the classical equations for Hφ produces identical results, i.e. no differences. The only differences between NEC and the equations appears to be in Ez due to the feedpoint voltage.

We can graph Ez and Hφ for a 40m λ/4 vertical as shown in figures C6 and C7. Io = 1Arms and both Ez and Hφ are at the ground surface, i.e. z=0.

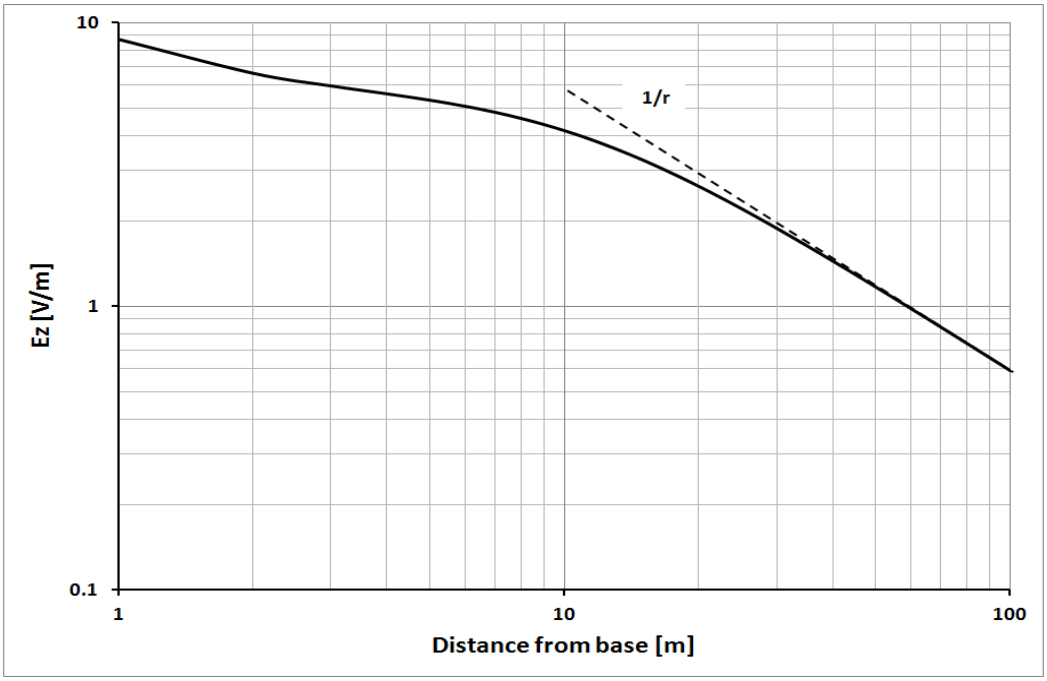

Figure C6 - Ez as a function of distance radially from a λ/4 vertical over perfect ground.

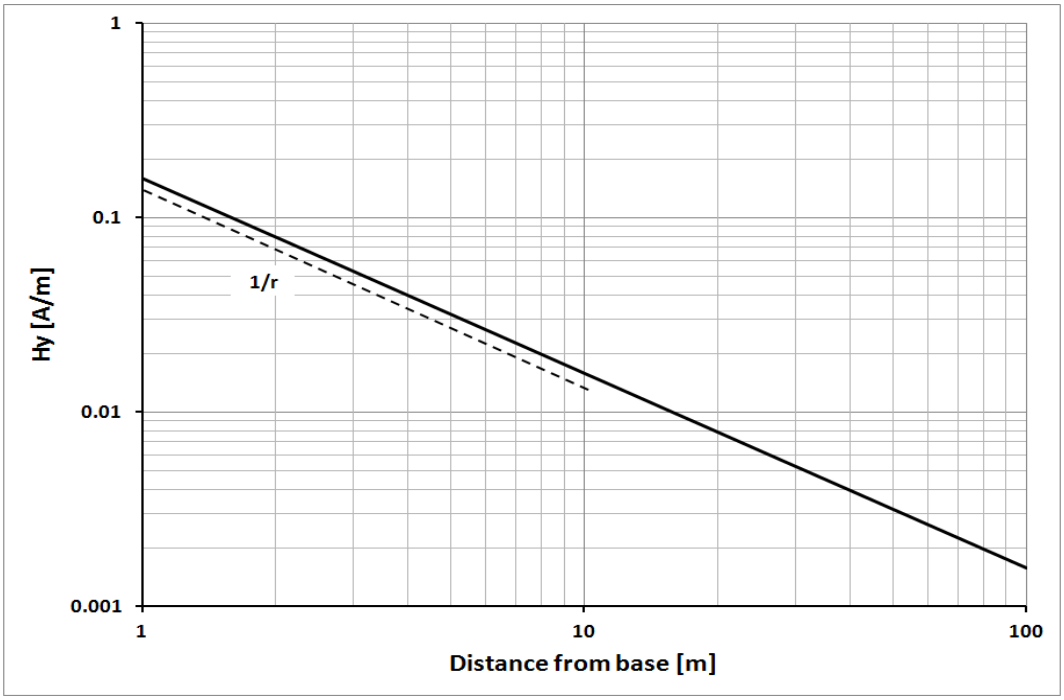

Figure C7- Hφ as a function of distance radially from a λ/4 vertical over perfect ground.

In figure C6 we see that Ez is asymptotic to 1/r for r>20m. As shown in figure C74 the H-field intensity decreases proportional to 1/r everywhere. In a radiation field (the far-

field) both Ez and Hφ decrease as 1/r. In this example this happens at ≈20m or 0.48λ. It appears that in the case of a λ/4 vertical setting the radius of the integration to ≈0.5λ (20m @ 7.2 MHz and 80m @ 1.8 MHz, etc) is reasonable. The slopes of the graphs in figures C6 and C7 agree with the predictions of equations (3) and (4).

Figures C6 and C7 are for a 40m λ/4 vertical. Ez and Hφ for a short (0.024λ) top-loaded 630m example behave differently with distance as shown in figures C8 and C9. What we see in these two graphs is good agreement with the predictions of equations (1) and (2) and figure C2.

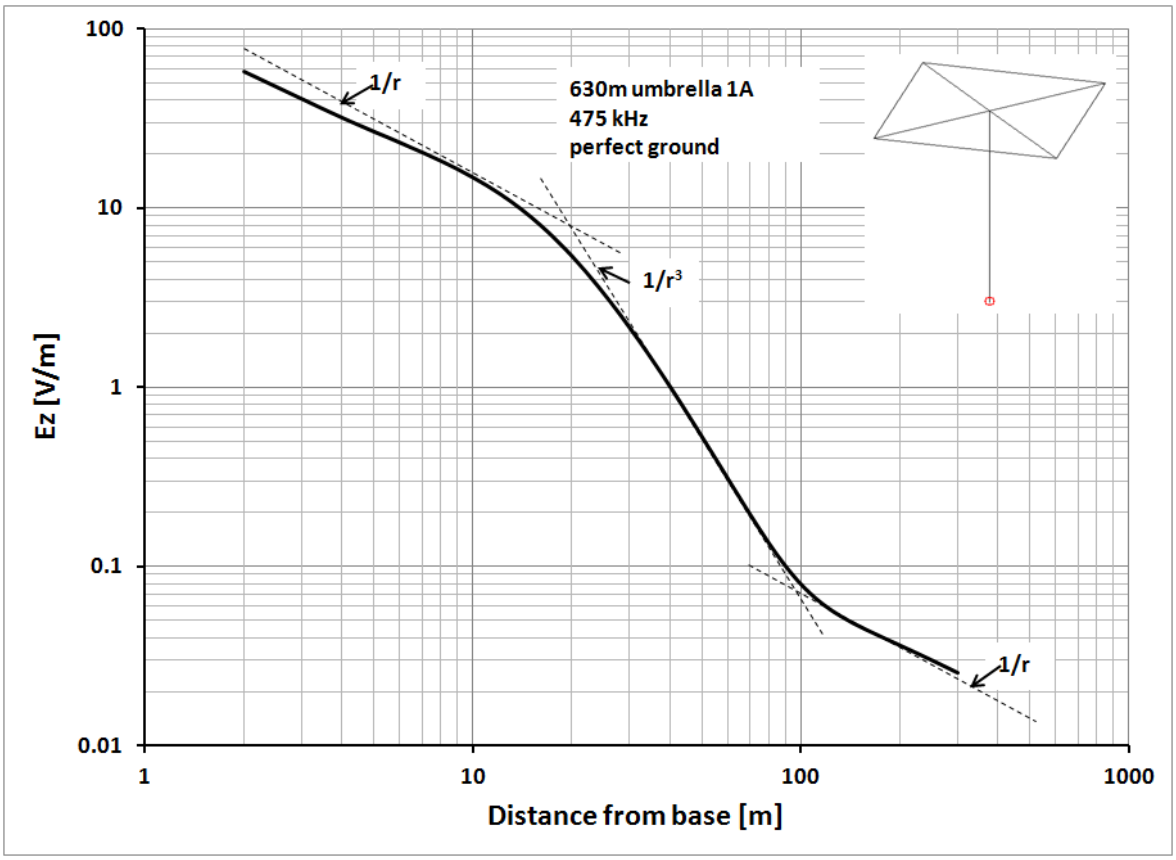

Figure C8 - Ez as a function of distance radially over perfect ground.

Near the base and under the top-hat Ez decreases ≈1/r but once out from under the hat the rate of decrease increases dramatically to ≈$1/r^3$. There is a corner at ≈ 100-120m where the rate of decrease with distance returns to 1/r. This fits the predictions in figure C3.

Hφ initially decreases ≈1/r but as we go beyond the hat Hφ begins dropping more rapidly (≈1/r^2). When we again reach a distance of ≈120m the rate of decrease slows to 1/r.

A rate of decrease of 1/r for both Ez and Hφ is what we would expect in the Fresnel and far fields which are radiation fields. These graphs indicate a change from a reactive field to a radiation field at a distance of ≈100m from the base of this antenna which suggests using 100m for the radius of the integration cylinder or disc.

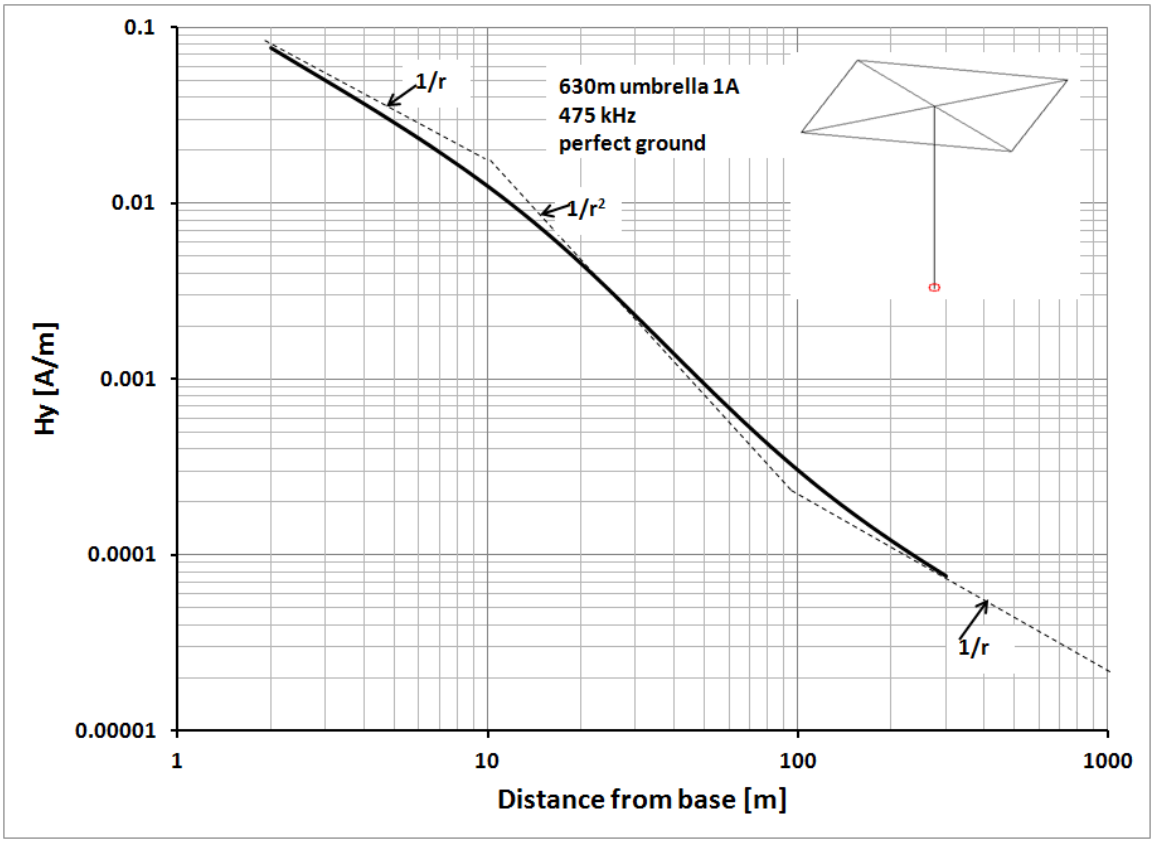

Figure C9 - Hφ as a function of distance radially over perfect ground.

The variation of |Ez| with distance from the base shown in figures C6 and C8 are for specific examples which appear in the article. We can expand this to include a range of antenna heights (h) as shown in figures C10 and C11. These are all simple monopoles without top-loading.

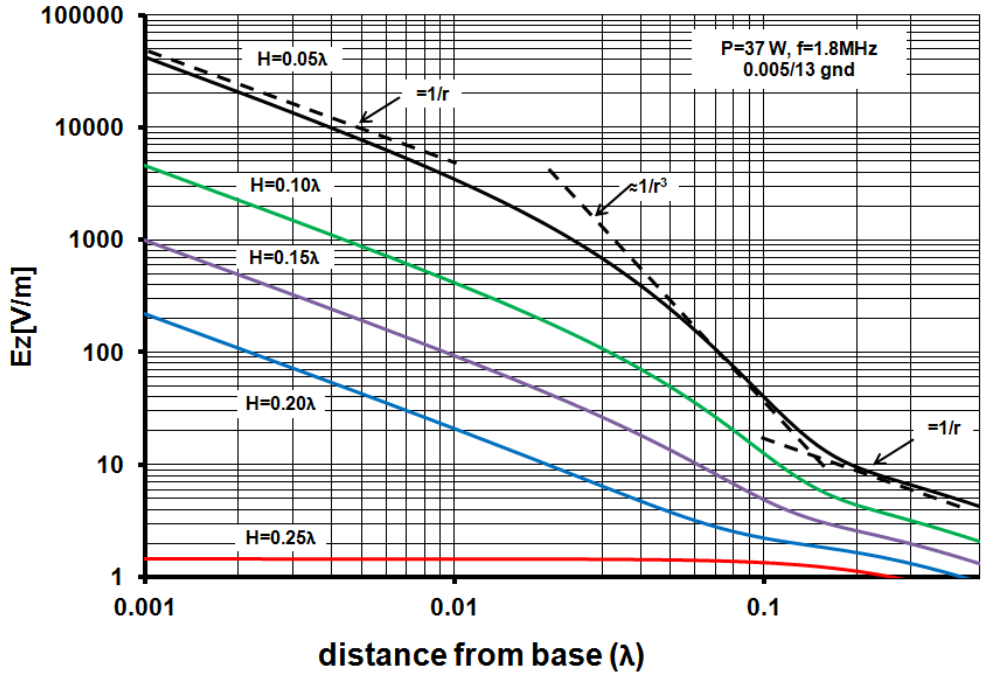

Figure C10 - A more general view of the variation in Ez with distance as a function of H.

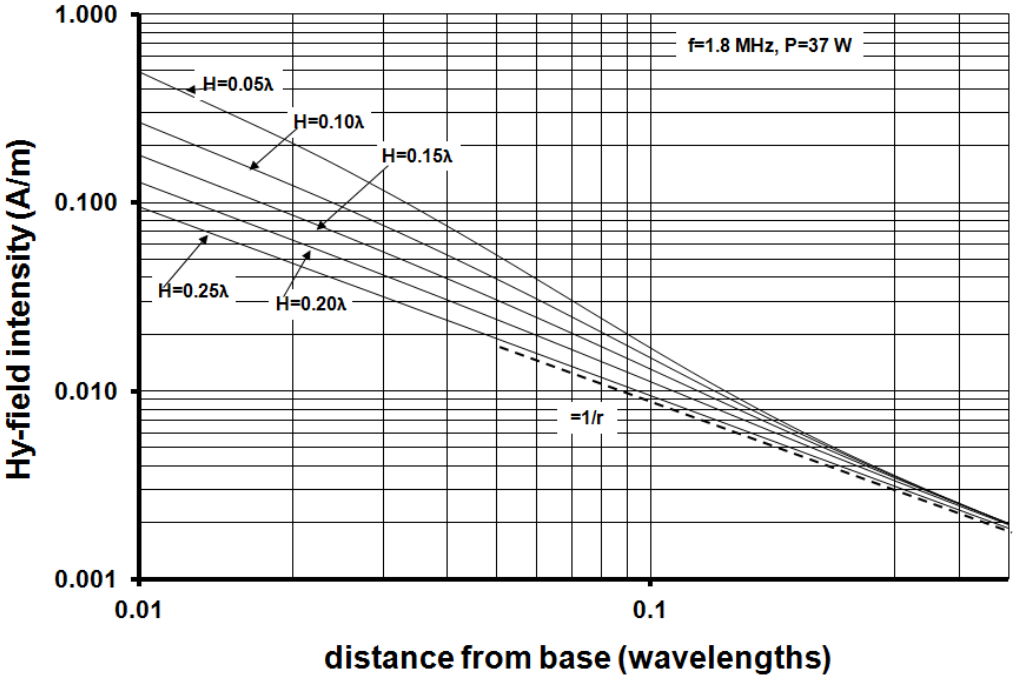

Figure C11 - Variation of Hφ with distance from the base.

The graph in figure C10 was generated using equations for the E-field intensity near a vertical. What we see is that the position of the "knee" (≈λ/8) is pretty much independent of H. Beyond the knee the slope is ≈1/r corresponding to a radiation field. The knee appears to be the boundary between the reactive near-field region and the

Fresnel region. In C11 the knee is not very obvious but by the time r>λ/8 the graphs are converging to a slope of 1/r.

E_z/H_y graphs

We can graph $|Ez|/|H_\varphi|$ at ground level (z=0) as a function of distance radially from the base. Figure C12 shows results for the 40m 0.25λ vertical. For a plane wave in free space $E_z/H_y=Z_o$= 376.8Ω. In figure C10 we can see that while at large distances E_z/H_y approaches 377 Ω there is no sharp distinction but by the time we reach 20m (≈λ/2) the ratio is converging rapidly on 377Ω.

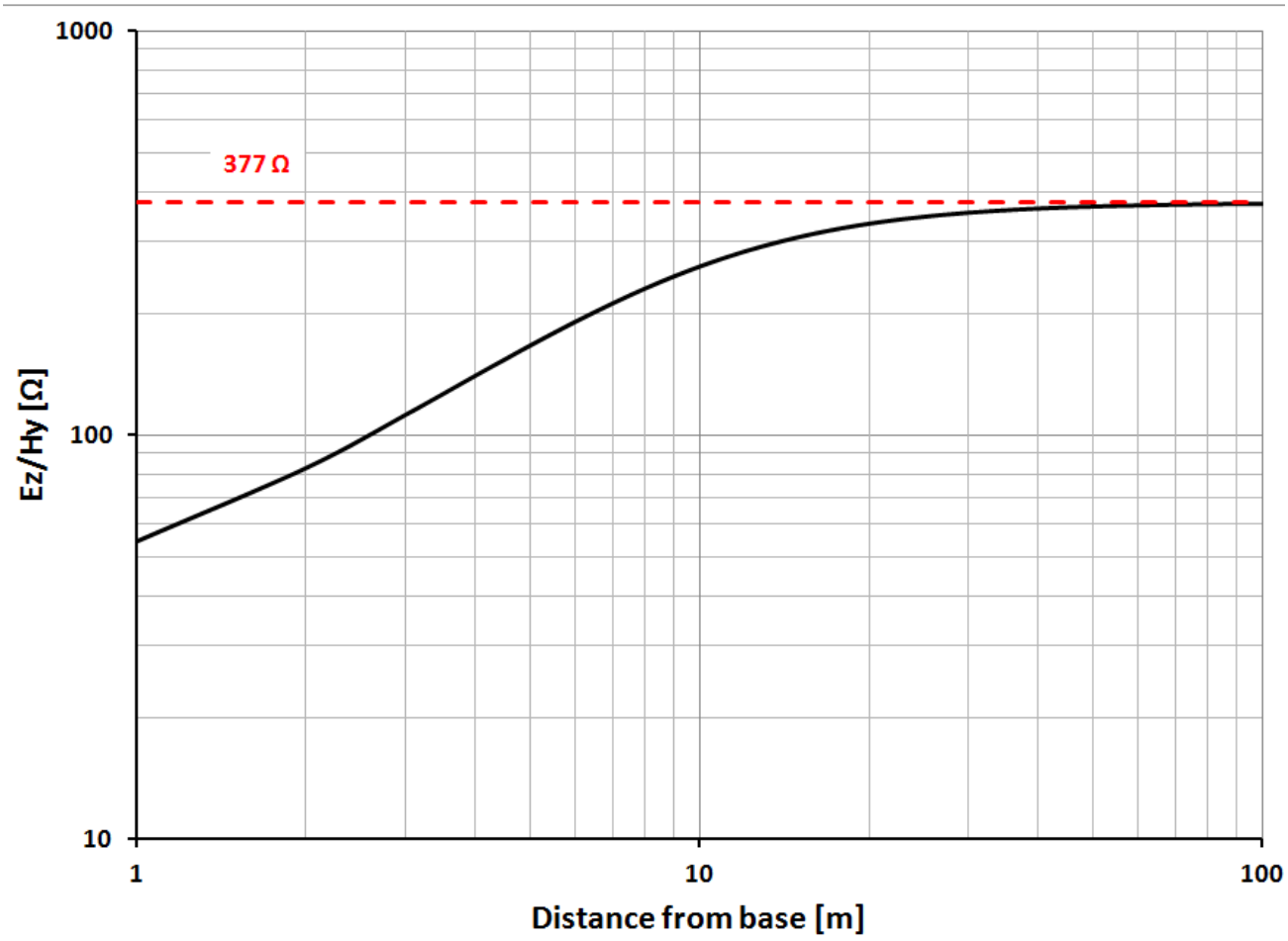

Figure C12 - Ez/Hφ radially for a λ/4 40m vertical over perfect ground.

A graph of E_z/H_y for the 630m antenna is shown in figure C13.

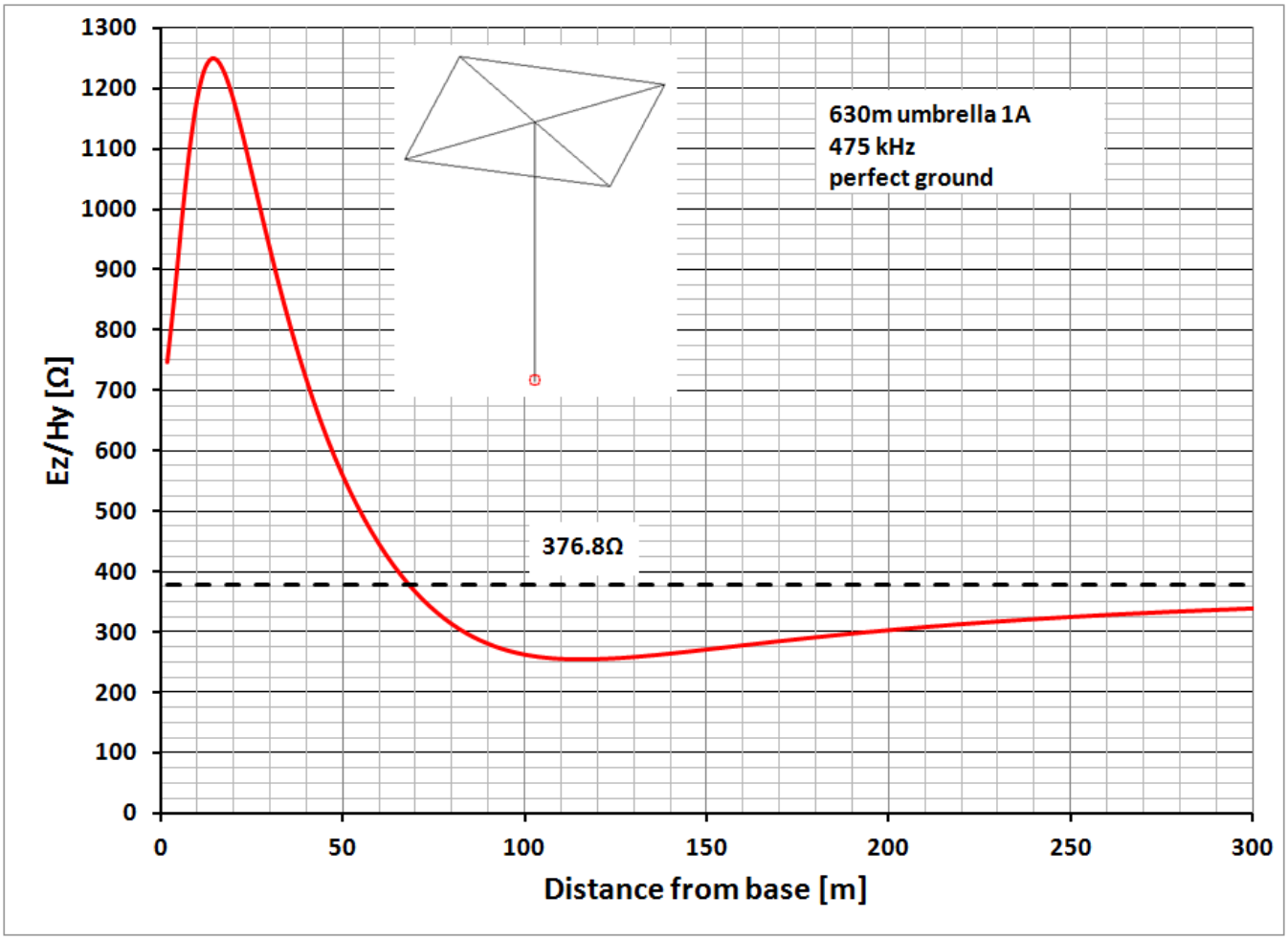

Figure C13 - Ezφ for the 0.024λ top-loaded 630m vertical.

Under the top-loading hat which extends out ≈8m the Ezφ impedance is very high but it quickly falls below 377 Ω and then slowly rises to asymptotically approach 376.8Ω. The minimum value occurs at r≈120m (≈400'). Again it would appear that something is happening around 100m or so. However, this minimum doesn't really pin down the outer radius of the reactive near-field very well. I think the field slopes shown in figures C8 and C9 are more definitive.

Varying the radius of the integration cylinder

We can vary the radius of the integration cylinder to see how calculated value for Rr is affected. Figure C14 is an example for a λ/4 vertical at 1.8 MHz over 0.005/13 soil, with sixty four 19m radials. The integration cylinder radius is varied from 20m to 160 m.

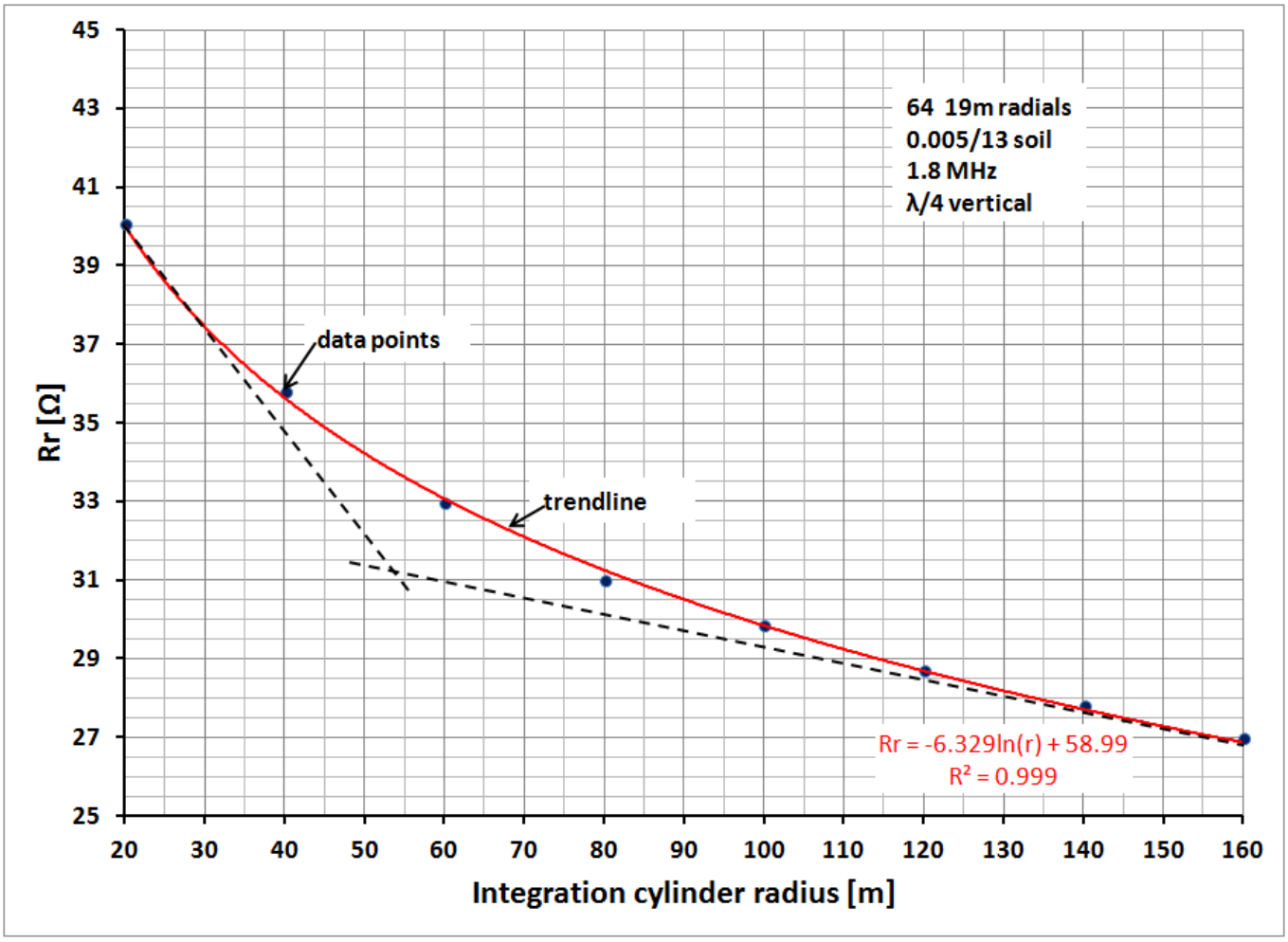

Figure C14 - Effect on Rr value from varying the integration cylinder radius.

By the time the integration cylinder radius reaches 80m (≈λ/2) the rate of change of **Rr** has begun to close in on its far-field value. Steve Stearns, K6OIK, has suggested to me that I extend the radius for figure C14 out to very large values to demonstrate how the value for Rr converges with a value for Rr derived from the average gain Ga. That's on my to-do list!

Total ground loss

There is yet another way to look for indications of region boundaries and that is to look at the total power loss in the soil within a given radius (r) without a ground system. Using equations from Watt[3] we can directly calculate the total power loss in the soil within a given radius. Figure C15 is an example for verticals of various heights at 1.8 MHz over 0.005/13 soil. The excitation current (**Io**) has been adjusted to provide a constant radiated power of 37W. For H=λ/4, Io=1Arms but for H=0.05λ Io=tbd Arms. The higher current in the shorter verticals results in much higher ground losses.

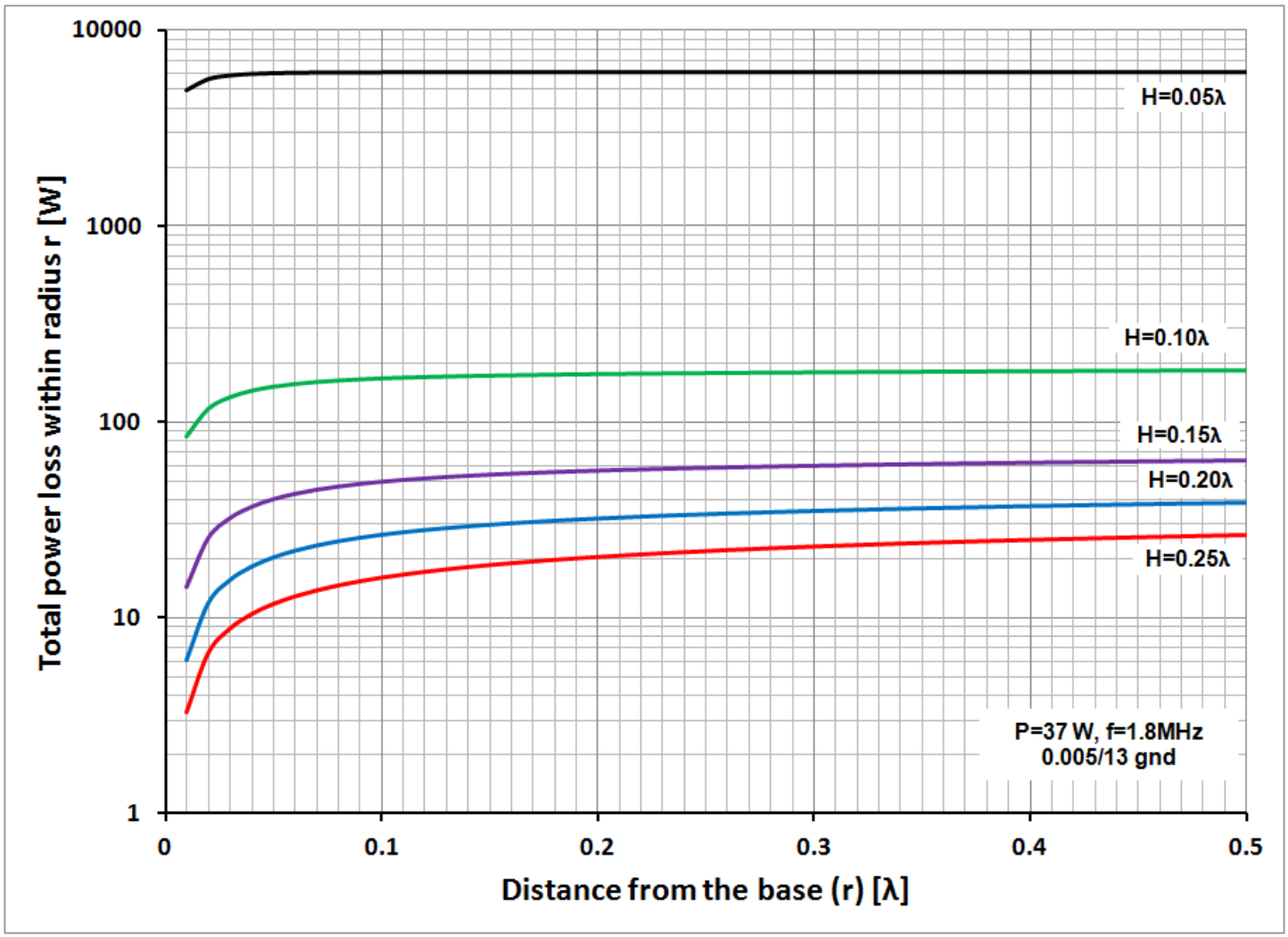

Figure C15 - Total power loss within a given radius r.

For H=0.25λ the total power loss rises most rapidly for r < 0.05λ but there is still a significant increase all the way out to r=0.5λ. For H=0.05λ the power loss also rises rapidly initially but then begins to flatten out for r>0.03λ. Using Balanis's boundaries for the reactive near field we get $R_1 \approx 0.22\lambda$ for a λ/4 vertical and $R_1 \approx 0.02\lambda$ for H=0.05λ. These boundaries are in reasonable agreement with figure C13 for the point at which the ground loss levels out.

However, we have to be a little careful here. The use of a logarithmic vertical scale can be deceiving, making the rate of change for 0.05λ appear to be much less than that for 0.25λ. To remedy this I've changed the scales to be linear with two different vertical axis as shown in figure C16. Both vertical axis have a range of 70W so we can compare the rate of change of power loss as a function of radius using the dashed straight lines on the graph. While the total power dissipation differs by over a factor of

over 200, the rate of increase for r>0.25 is very similar, suggesting we're getting out into the radiation field.

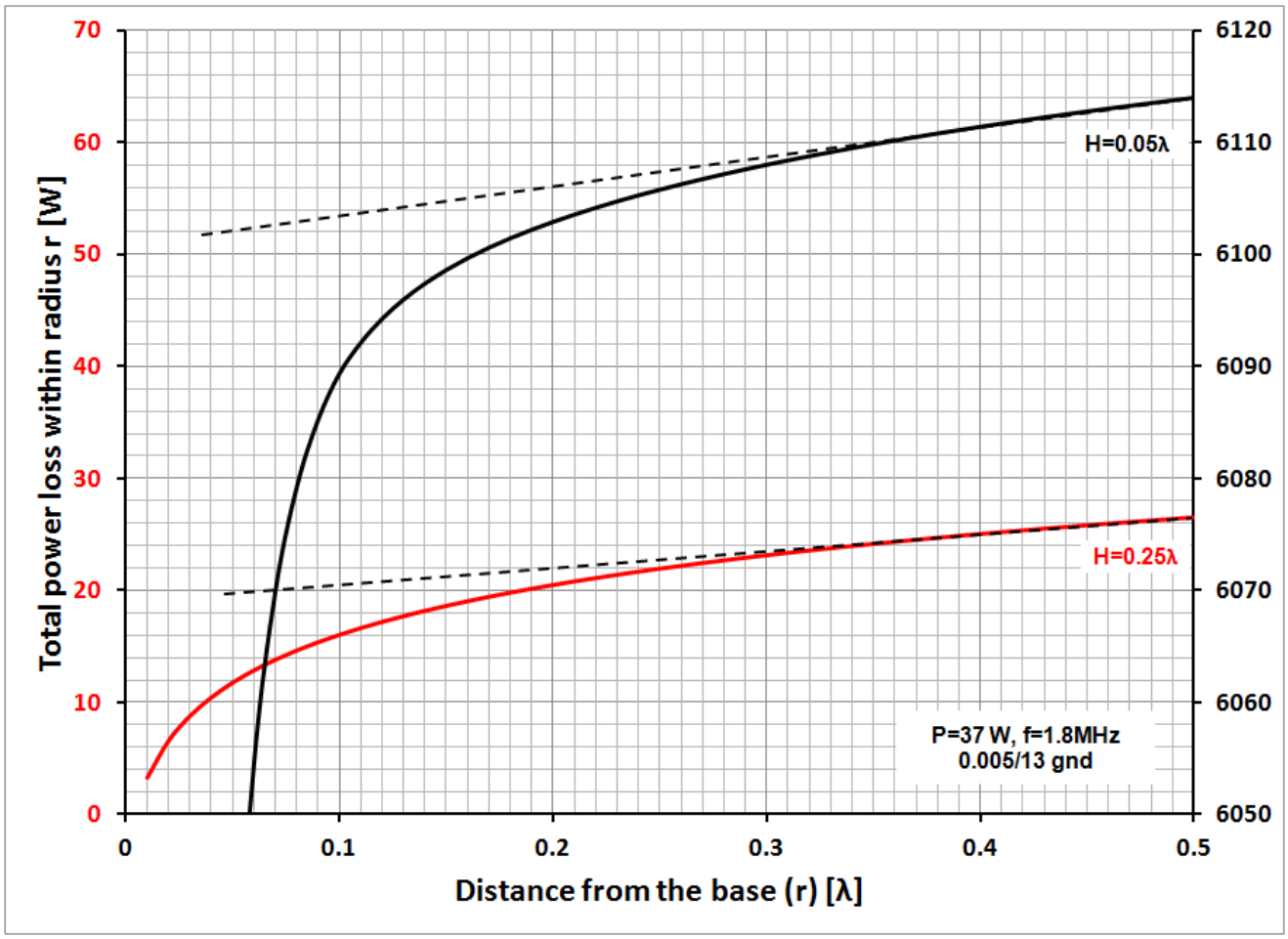

Figure C16 - Expanded scale version of figure C13.

Summary

As a practical matter λ/2 radials are pretty much the longest seen in practice. Radial lengths up to 0.4-0.5 λ are recognized as being into the region of vanishing returns as far as reducing **Rg** is concerned. Typically, λ/4 radials are used with λ/4 verticals and for very short verticals the radials are usually only a little longer than the height of the vertical but usually much more numerous.

Given all the forgoing discussion, the radius for the integration cylinder is still rather arbitrary. For this work I chose to use a radius of λ/2 for both the 1.8 and 7.2 MHz verticals and 100m or 0.16λ for the 630m vertical as reasonable compromises. While my choices for integration cylinder radius may not provide a definitive number for **Rr** they still illustrate that for a given integration radius **Rr** is not some fixed number but varies with the soil characteristics, radial number and length, etc.

References

[1] John Kraus, Antennas, second edition, McGraw-Hill, 1988

[2] Constantine Balanis, Antenna Theory Analysis and Design, Harper and Row, 1982

[3] Arthur Watt, VLF Radio Engineering, Pergamon Press, 1967, see section 2.4